Journal of Organometallic Chemistry, 370 (1989) 187–202
Elsevier Sequoia S.A., Lausanne – Printed in The Netherlands
JOM 09815

Enantioselective hydrogen transfer reactions from propan-2-ol to ketones catalyzed by pentacoordinate iridium(I) complexes with chiral Schiff bases

Grazia Zassinovich, Roberto Bettella, Giovanni Mestroni, Nevenka Bresciani-Pahor, Silvano Geremia and Lucio Randaccio

Dipartimento di Scienze Chimiche, Università di Trieste, Piazzale Europa 1, 34127 Trieste (Italy)

(Received October 31st, 1988)

Abstract

Some diastereoisomeric pentacoordinate complexes of the type [Ir(COD)-(NNR*)I] (COD = *cis,cis*-1,5-cyclooctadiene; NNR* = 2-pyridinal-1-phenylethylimine (PPEI) (I), 2-acetylpyridine-1-phenylethylimine (APPEI) (II)) have been synthesized. The complexes are active and selective catalysts for asymmetric hydrogen transfer from propan-2-ol to prochiral ketones. Optical yields of up to 84% have been obtained in the reduction of t-butyl phenyl ketone. The structure and absolute configuration of complexes I and II were determined by X-ray diffraction.

Introduction

Asymmetric catalytic reductions of prochiral ketones can be readily brought about through hydrogenation, hydrosilylation and hydrogen transfer reactions. The effective catalysts for these reactions are mainly Rh^I and Ir^I complexes with chiral phosphine, sulfoxide, or nitrogen donor bidentate ligands [1–11].

High enantiomeric excesses (> 90%) have been obtained in the case of hydrosilylation reactions promoted by Rh^I complexes with bi- and ter-dentate chiral nitrogen donor ligands, although the reaction is rather slow [8,9]. On the other hand, high reaction rates have been obtained using Ir^I cationic derivatives with chiral bidentate Schiff bases as catalysts, but up to now optical yields of only up to 50% have been achieved [6].

We previously reported [12] that the reduction of 4-t-butylcyclohexanone by propan-2-ol is more selective when [Ir(HD)(chel)I] (HD = 1,5 hexadiene; chel = 1,10-phenanthroline and their substituted derivatives) are used instead of the corresponding tetracoordinated cationic derivatives as catalyst precursors. Selectivities for the *trans* alcohol of up to 97% have been obtained. We thus decided to try the pentacoordinate neutral complexes of the type [Ir(COD)(NNR*)I] (COD =

0022-328X/89/$03.50 © 1989 Elsevier Sequoia S.A.

cis,cis-1,5-cyclooctadiene; NNR* = chiral pyridinimines) as catalyst precursors in the asymmetric reduction of prochiral ketones.

We present here the results of an X-ray structural analysis of two pentacoordinated [Ir(COD)(NNR*)I] species (NNR* = 2-pyridinal-1-phenylethylimine = PPEI (I); 2-acetylpyridine-1-phenylethylimine = APPEI (II)) and data on the catalytic activities and the enantioselectivities of these complexes in hydrogen transfer from propan-2-ol to alkyl phenyl ketones, and compare the results with those obtained with the corresponding [Ir(COD)(PPEI)]ClO_4 (III) and [Ir(COD)(APPEI)]ClO_4 (IV) derivatives.

Synthesis and structural characterization

The Schiff bases used can be readily synthesized by condensation of the carbonyl compound with *R*(+)- or *S*(−)-1-phenylethylamine [13,7]. The complexes [Ir(COD)(NNR*)I] are prepared by treating a methanolic solution of $[Ir(COD)Cl]_2$ with a slight excess of the ligand, followed by addition of solid NaI. Each iodo derivative can exist as a diastereoisomeric pair differing only in the absolute configuration, *R* or *S*, of the asymmetric iridium atom; recrystallization from $CHCl_3$/ligroin (NNR* = PPEI) or CH_2Cl_2/ligroin (NNR* = APPEI) give only one diastereoisomer. The structural X-ray analysis was performed on single crystals of the compounds obtained using *S*(+)PPEI and *S*(+)APPEI.

Cell dimensions of I and II, determined from Weissenberg and precession photographs, were refined on a CAD4 Enraf–Nonius single crystal diffractometer.

Table 1

Details of the crystallographic procedure for compounds I and II

Formula	I $IrIN_2C_{22}H_{26}$	II $IrIN_2C_{23}H_{28}$
Mw	637.6	651.6
a, Å	7.420(1)	10.353(2)
b, Å	10.317(2)	10.353(2)
c, Å	27.461(4)	40.673(8)
D_m, g cm^{-3}	2.00	2.00
D_c, g cm^{-3}	2.01	1.99
Z	4	8
Space group	$P2_12_12_1$	$P4_32_12$
μ(Mo-K_α), cm^{-1}	77.9	75.1
cryst. dimens., cm	0.01×0.03×0.05	0.01×0.02×0.03
%transmission/min,max	58.9, 99.8	69.8, 99.7
max 2θ(Mo-K_α), deg	56	60
scan angle, deg	1.2+0.35 tan θ	1.0+0.35 tan θ
no. meas. reflections	2900	3797
no. indep. reflections $I \geqslant 3\sigma(I)$	2144	2400
R^+	0.035	0.032
R_w^+	0.045	0.038
goodness of fit	1.00	0.92
$w = 1/(\sigma^2(F)+(0.02F)^2+q)$	$q = 3$	$q = 1$
max,min density in difference map	0.89, 0.87	1.03, 0.55

The results are given in Table 1. The intensities were collected by the θ–2θ scan technique using graphite-monochromated Mo-K_α radiation. Three standard reflections measured every 60 min showed no systematic variation throughout the data collections. Reflections having intensities $I \geq 3\sigma(I)$ were corrected for Lorentz and polarization effects and for absorption via ψ scan (see Table 1).

Both structures were solved by conventional Patterson and Fourier methods and refined by the full-matrix anisotropic least-squares method. In the final cycles the hydrogen atoms were included at calculated positions (held constant at $B = 1.3B_{eq}$ (Å^2), where B_{eq} is the equivalent thermal factor of the atom to which each is bonded). The final R^+ and R_w^+ factors and weighting schemes are given in Table 1. Refinement with the signs of if'' reversed (or with inverted coordinates for I and inverted coordinates in the enantiomorphic space group $P4_12_12$ for II) gave $R^- = 0.057$, $R_w^- = 0.070$ for I and $R^- = 0.047$, $R_w^- = 0.058$ for II. The values $\mathscr{R} = R_w^-/R_w^+ = 1.56$ (I) and 1.53 (II) confirm the correct assignment of absolute configuration [14]. Neutral atom scattering factors and anomalous-dispersion correction terms were taken from ref. 15. All the calculations were carried out on a PDP11/44

Table 2

Atomic coordinates for non-hydrogen atoms (with esd's in parentheses) for I and II [a]

Atom	I				II			
	x	y	z	B (Å^2)	x	y	z	B (Å^2)
Ir	0.37662(8)	0.06513(5)	0.14994(2)	2.977(7)	0.19492(3)	0.71249(4)	0.94479(1)	2.808(6)
I	0.7088(2)	0.0273(1)	0.19920(5)	4.84(2)	0.20601(8)	0.74240(8)	1.01433(2)	4.23(1)
N1	0.317(1)	−0.131(1)	0.1608(4)	3.4(2)	0.3966(7)	0.7114(9)	0.9456(2)	3.3(2)
N2	0.252(1)	0.064(1)	0.2186(4)	2.6(2)	0.238(1)	0.5179(8)	0.9508(2)	3.9(2)
C1	0.355(2)	−0.244(1)	0.1271(6)	3.8(3)	0.474(1)	0.832(1)	0.9442(3)	3.8(2)
C2	0.432(2)	−0.364(2)	0.1524(8)	6.8(4)	0.550(1)	0.856(2)	0.9757(3)	6.3(3)
C3	0.192(2)	−0.271(1)	0.0972(5)	3.2(3)	0.547(1)	0.846(1)	0.9116(3)	3.5(2)
C4	0.028(2)	−0.203(1)	0.0998(5)	3.7(3)	0.523(1)	0.762(1)	0.8854(3)	4.2(3)
C5	−0.115(3)	−0.237(2)	0.0712(6)	5.2(4)	0.588(1)	0.779(1)	0.8556(3)	4.6(3)
C6	−0.105(3)	−0.337(2)	0.0395(7)	8.5(5)	0.675(1)	0.876(1)	0.8520(3)	4.4(3)
C7	0.050(4)	−0.406(2)	0.0366(7)	8.4(6)	0.696(1)	0.961(1)	0.8776(3)	4.9(3)
C8	0.200(3)	−0.375(2)	0.0639(7)	6.1(5)	0.634(1)	0.945(1)	0.9078(3)	3.8(2)
C9	0.254(2)	−0.160(1)	0.2033(5)	3.4(3)	0.452(1)	0.599(1)	0.9492(2)	3.3(2)
C10	0.216(2)	−0.056(1)	0.2367(5)	3.3(2)	0.365(1)	0.489(1)	0.9524(2)	3.6(2)
C11	0.147(2)	−0.074(2)	0.2830(5)	4.2(3)	0.411(2)	0.362(1)	0.9569(3)	5.7(3)
C12	0.105(2)	0.034(2)	0.3109(6)	4.8(4)	0.316(2)	0.265(1)	0.9599(3)	7.0(4)
C13	0.144(2)	0.155(1)	0.2927(5)	3.7(3)	0.191(2)	0.298(1)	0.9585(3)	7.4(4)
C14	0.220(2)	0.167(1)	0.2469(6)	3.6(3)	0.152(1)	0.422(1)	0.9537(3)	5.9(3)
C15	0.422(3)	0.269(2)	0.1432(6)	5.2(4)	−0.007(1)	0.698(1)	0.9439(3)	5.5(3)
C16	0.240(3)	0.241(1)	0.1329(7)	5.4(4)	0.040(1)	0.659(1)	0.9126(3)	5.1(3)
C17	0.170(3)	0.241(3)	0.0803(8)	8.1(6)	0.028(2)	0.736(2)	0.8820(3)	7.5(4)
C18	0.210(5)	0.131(3)	0.0501(8)	12(1)	0.112(2)	0.850(2)	0.8816(3)	8.8(5)
C19	0.334(3)	0.041(2)	0.0737(5)	5.2(4)	0.193(1)	0.870(1)	0.9106(3)	4.4(2)
C20	0.511(3)	0.063(2)	0.0812(6)	5.7(4)	0.150(1)	0.914(1)	0.9419(3)	4.3(2)
C21	0.615(4)	0.193(2)	0.0725(9)	9.9(6)	0.007(1)	0.938(2)	0.9492(5)	8.5(4)
C22	0.563(3)	0.299(2)	0.1047(7)	5.8(5)	−0.073(1)	0.825(2)	0.9510(4)	7.8(4)
C23					0.595(1)	0.574(2)	0.9490(3)	5.8(3)

[a] Anisotropically refined atoms are given in the form of the isotropic equivalent thermal parameter defined as: $\frac{4}{3}[a^2B_{1,1} + b^2B_{2,2} + c^2B_{3,3} + ab(\cos\gamma)B_{1,2} + ac(\cos\beta)B_{1,3} + bc(\cos\alpha)B_{2,3}]$.

computer using programs from the SDP-CAD4 package. Final non-hydrogen atomic parameters are given in Table 2. Tables of hydrogen atom coordinates, anisotropic thermal parameters, and a list of observed and calculated structure factors are available from the authors.

Description and discussion of structures I and II

The final refinements (see above) showed unequivocally that in the crystals the absolute configuration is *S* at the Ir atom and *S* at the asymmetric carbon atom for both I and II. As expected, both compounds are formed with retention of the configuration at the asymmetric carbon atom. For the specification of the Ir configuration the priority sequence COD > N(imine) > N(pyridine) > I was used [16–18]. The ORTEP drawings for compounds I and II with the numbering schemes for the atoms are given in Figs. 1 and 2. The bond lengths and angles are listed in Tables 3 and 4. In both I and II the Ir atom has a distorted square pyramidal geometry, with the iodine atom in the apical position. The basal positions are occupied by the bidentate NNR* and COD ligands. In both compounds the latter is coordinated in such a way that its C(15) and C(20) atoms nearly lie in the N1,N2,Ir plane (see Figs. 1 and 2), while C(16) and C(19) are below this plane, i.e. on the side opposite to that of I, with very similar Ir–C distances (Table 3 and 4). The overall conformation of the 1-phenylethyl group with the H atom bonded to C(1) pointing towards Ir in both I and II, confirms the previous finding [19] that the interaction of this group with the substituent at the imino carbon atom C(9) is not the only conformation-determining effect [20]. Interaction of the substituents on the asymmetric carbon atom with the COD ligand plays an important role.

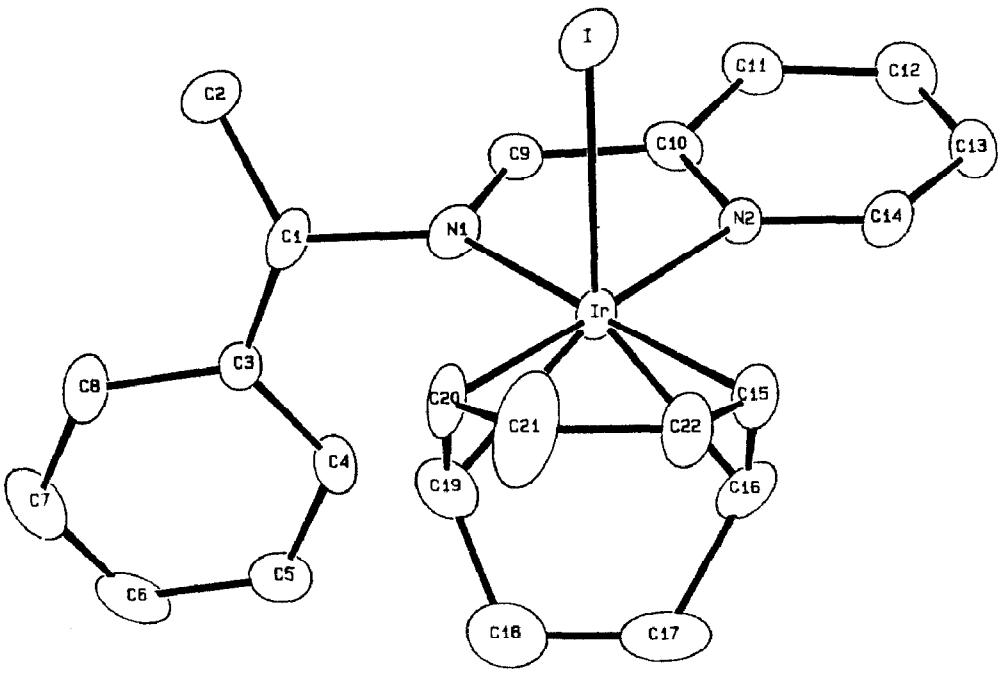

Fig. 1. ORTEP drawing and labeling scheme for non-hydrogen atoms of I.

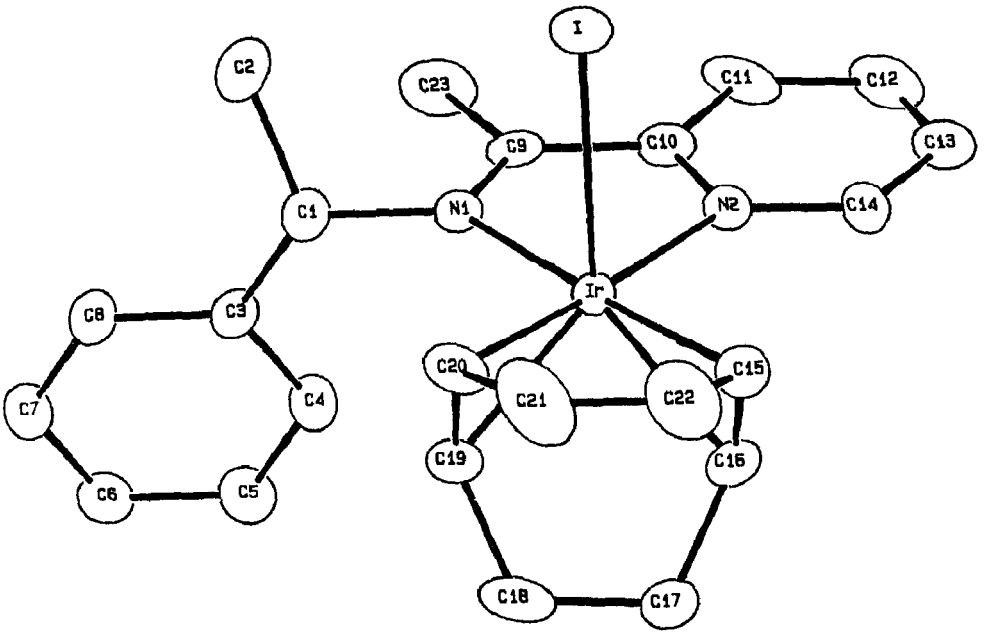

Fig. 2. ORTEP drawing and labeling scheme for non-hydrogen atoms of II.

Table 3

Bond lengths (Å) and angles (°) with esd's in parentheses, for I

Ir–I	2.839(1)	C1–C2	1.54(2)	C12–C13	1.38(2)
Ir–N1	2.09(2)	C1–C3	1.49(2)	C13–C14	1.38(3)
Ir–N2	2.100(9)	C3–C4	1.40(2)	C15–C16	1.42(3)
Ir–C15	2.14(2)	C3–C8	1.41(2)	C15–C22	1.52(3)
Ir–C16	2.14(2)	C4–C5	1.37(2)	C16–C17	1.53(3)
Ir–C19	2.13(1)	C5–C6	1.35(3)	C17–C18	1.44(4)
Ir–C20	2.13(2)	C6–C7	1.36(4)	C18–C19	1.45(4)
N1–C1	1.52(2)	C7–C8	1.38(3)	C19–C20	1.35(3)
N1–C9	1.30(2)	C9–C10	1.44(2)	C20–C21	1.57(3)
N2–C10	1.36(2)	C10–C11	1.39(2)	C21–C22	1.47(3)
N2–C14	1.34(2)	C11–C12	1.39(2)		
I–Ir–N1	88.9(4)	Ir–N1–C1	128.0(9)	C10–C11–C12	119(2)
I–Ir–N2	87.3(3)	Ir–N1–C9	115.3(9)	C11–C12–C13	119(1)
I–Ir–C15	92.3(5)	C1–N1–C9	116(1)	C12–C13–C14	120(1)
I–Ir–C16	129.4(5)	Ir–N2–C10	114.7(8)	N2–C14–C13	122(1)
I–Ir–C19	125.6(6)	Ir–N2–C14	126.8(9)	Ir–C15–C16	70.8(9)
I–Ir–C20	90.9(6)	C10–N2–C14	118(2)	Ir–C15–C22	112(1)
N1–Ir–N2	76.9(5)	N1–C1–C2	115(1)	C16–C15–C22	125(2)
N1–Ir–C15	175.6(6)	N1–C1–C3	109(1)	Ir–C16–C15	71(1)
N1–Ir–C16	139.0(6)	C2–C1–C3	113(1)	Ir–C16–C17	111(1)
N1–Ir–C19	89.8(6)	C1–C3–C4	126(1)	C15–C16–C17	121(2)
N1–Ir–C20	102.3(5)	C1–C3–C8	118(1)	C16–C17–C18	118(3)
N2–Ir–C15	98.8(6)	C4–C3–C8	117(1)	C17–C18–C19	112(2)
N2–Ir–C16	89.6(6)	C3–C4–C5	121(1)	Ir–C19–C18	117(1)
Nr–Ir–C19	144.6(6)	C4–C5–C6	122(2)	Ir–C19–C20	72(1)
N2–Ir–C20	178.1(6)	C5–C6–C7	119(2)	C18–C19–C20	126(3)
C15–Ir–C16	38.6(7)	C6–C7–C8	122(2)	Ir–C20–C19	71(2)
C15–Ir–C19	93.0(8)	C3–C8–C7	120(2)	Ir–C20–C21	111(1)
C15–Ir–C20	82.0(6)	N1–C9–C10	118(1)	C19–C20–C21	127(2)
C16–Ir–C19	79.2(8)	N2–C10–C9	115(1)	C20–C21–C22	115(3)
C16–Ir–C20	92.2(7)	N2–C10–C11	122(1)	C15–C22–C21	117(2)
C19–Ir–C20	36.9(7)	C9–C10–C11	124(1)		

Table 4

Bond lengths (Å) and angles (°), with esd's in parentheses, for II

Ir–I	2.8476(7)	C1–C2	1.53(2)	C11–C12	1.41(2)
Ir–N1	2.088(8)	C1–C3	1.53(1)	C12–C13	1.34(3)
Ir–N2	2.079(9)	C3–C4	1.40(2)	C13–C14	1.36(2)
Ir–C15	2.11(2)	C3–C8	1.37(2)	C15–C16	1.42(2)
Ir–C16	2.14(1)	C4–C5	1.39(2)	C15–C22	1.52(2)
Ir–C19	2.15(1)	C5–C6	1.36(2)	C16–C17	1.48(2)
Ir–C20	2.14(2)	C6–C7	1.38(2)	C17–C18	1.48(2)
N1–C1	1.49(1)	C7–C8	1.40(2)	C18–C19	1.46(2)
N1–C9	1.31(1)	C9–C10	1.46(2)	C19–C20	1.42(2)
N2–C10	1.35(2)	C9–C23	1.51(2)	C20–C21	1.53(2)
N2–C14	1.34(2)	C10–C11	1.41(2)	C21–C22	1.43(2)
I–Ir–N1	86.9(2)	Ir–N1–C9	116.6(8)	C10–C11–C12	116(1)
I–Ir–N2	88.8(2)	C1–N1–C9	121.0(8)	C11–C12–C13	119(1)
I–Ir–C15	93.7(4)	Ir–N2–C10	115.7(8)	C12–C13–C14	122(1)
I–Ir–C16	131.7(3)	Ir–N2–C14	125.8(9)	N2–C14–C13	121(1)
I–Ir–C19	124.2(3)	C10–N2–C14	118(1)	Ir–C15–C16	72.0(7)
I–Ir–C20	87.6(4)	N1–C1–C2	113(1)	Ir–C15–C22	112.4(9)
N1–Ir–N2	77.2(4)	N1–C1–C3	112.5(9)	C16–C15–C22	125(1)
N1–Ir–C15	175.6(5)	C2–C1–C3	116.9(9)	Ir–C16–C15	68.8(7)
N1–Ir–C16	139.2(4)	C1–C3–C4	121(1)	Ir–C16–C17	117(1)
N1–Ir–C19	91.5(5)	C1–C3–C8	120(1)	C15–C16–C17	126(1)
N1–Ir–C20	103.0(4)	C4–C3–C8	120(2)	C16–C17–C18	113(1)
N2–Ir–C15	98.5(5)	C3–C4–C5	121(2)	C17–C18–C19	116(1)
N2–Ir–C16	89.2(5)	C4–C5–C6	120(2)	Ir–C19–C18	116(1)
N2–Ir–C19	144.8(4)	C5–C6–C7	120(2)	Ir–C19–C20	70.5(6)
N2–Ir–C20	176.4(4)	C6–C7–C8	121(1)	C18–C19–C20	126(1)
C15–Ir–C16	39.1(5)	C3–C8–C7	120(2)	Ir–C20–C19	70.9(6)
C15–Ir–C19	91.8(6)	N1–C9–C10	115.7(9)	Ir–C20–C21	111.0(9)
C15–Ir–C20	81.4(6)	N1–C9–C23	126(2)	C19–C20–C21	122(1)
C16–Ir–C19	78.0(5)	C10–C9–C23	118(2)	C20–C21–C22	116(1)
C16–Ir–C20	93.1(5)	N2–C10–C9	114.9(9)	C15–C22–C21	116(1)
C19–Ir–C20	38.7(4)	N2–C10–C11	123(1)		
Ir–N1–C1	122.3(7)	C9–C10–C11	122(1)		

The only relevant differences between I and II are ascribable to the methyl substituent at C(9) in the latter. Thus the C(1)–N(1)–C(9) angle is 116(1)° in I and 121.1(8)° in II, while the Ir–N(1)–C(1) angle is 128.0(9) and 122.3(7)° in I and II, respectively. Furthermore, comparison of the torsional angles around the N(1)–C(1) bond in I and II shows that these angles are clearly affected by the presence of the C(23) methyl group, as shown in Fig. 3, in which the side views of the molecules along the C(1)–N(1) bond are shown. In I the H atom of the 1-phenylethyl group is slightly but significantly above the plane of the bidentate Schiff base, on the side of the iodine atom, while in II it lies essentially in this plane. Correspondingly, the phenyl group in II is further away from COD than in I, and the dihedral angle between its mean plane and the mean plane of the chelate ring is reduced from 90° in I to 76° in II (see Fig. 3). The parameters suggested by Brunner et al. [19] to define the conformation of the 1-phenylethyl group in the chelate ligand are given in Table 5. For comparison, in the same Table the corresponding parameters of the closely related Rh tetracoordinate complex [Rh(COD)(*S*)PCPE], where (*S*)PCPE =

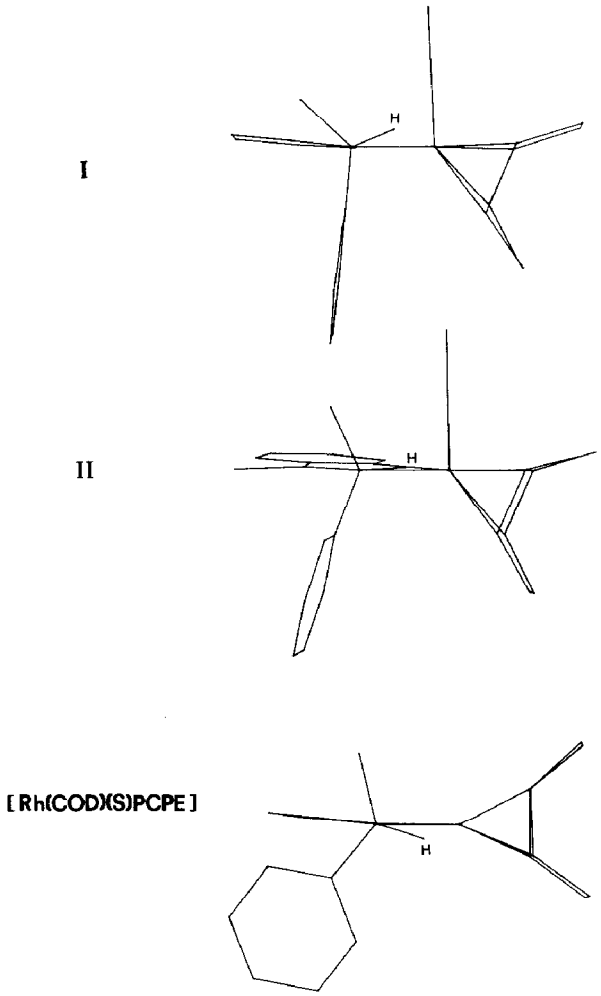

Fig. 3. Side view of the molecules along the C(1)–N(1) bond for I, II and [Rh(COD)(*S*)PCPE].

pyrrol-2-carbaldehyd-(*S*)-1-phenylethyliminato, are also given. The view along the C(1)–N(1) bond for the latter is given in Fig. 3. Comparison of the side views in Fig. 3 shows that COD is "asymmetrically" coordinated in I and II (see above), whereas

Table 5

Parameters defining the conformation of the 1-phenylethyl group for I, II and [Rh(COD)(*S*)PCPE]

	I	II	[Rh(COD)(*S*)PCPE]
M–N(1) (Å)	2.09(2)	2.088(8)	2.119(4)
N(1)–C(1) (Å)	1.52(2)	1.49(1)	1.492(7)
N(1)–M–N(2) (°)	76.9(5)	77.2(4)	78.9(2)
M–N(1)–C(1) (°)	128.0(9)	122.3(7)	128.9(4)
N(2)–M–B(1)–C(1) (°)	180(1)	−176.5(7)	179.2
M–N(1)–C(1)–C(2) (°)	136(1)	114.7(9)	104.5
M–N(1)–C(1)–C(3) (°)	−95(1)	−110.8(8)	−128.1
M–N(1)–C(1)–H (°)	23	4	−17.3
N(1)–C(1)–C(3)–C(4) (°)	0(2)	9(1)	77.6

it is "symmetrically" coordinated in the tetracoordinate Rh complex. This difference is clearly due to the presence of the apical I atom. Furthermore, the orientation of the phenyl group is different in the Rh complex from that in I and II; the relevant torsion angle (see Table 5) is 77.6° for the Rh complex compared with 0° in I and 9° in II. The different orientation of the phenyl group may be responsible for the slightly different conformation of the 1-phenylethyl group in the Rh compound, where the H atom bonded to C(1) is out of the chelate plane, as in I, but on the opposite side. Probably, in I and II the "asymmetrically" coordinated COD and the apical I atom, which would interact sterically with the substituents at C(1), prevent the phenyl group assuming the orientation found in the Rh compound.

Catalytic activity

The studied reaction is reported in Scheme 1. Propan-2-ol was used as hydrogen donor and as solvent. To become catalytically active, the complexes require activation and the presence of a basic cocatalyst (KOH) [5,6].

Both the activity and selectivity of the reaction depend on many variables, among them the concentrations of potassium hydroxide and water, and, of course, the nature of the chiral ligands and of the prochiral substrates.

Table 6 shows the results obtained with [Ir(COD)(PPEI)I] and [Ir(COD)(PPEI)]-ClO_4 as catalyst precursors and t-butylphenyl ketone as substrate.

The pentacoordinate derivative is less active, but significantly more selective, than the corresponding tetracoordinate complex (66.% e.e. versus 50.% e.e.). Shorter reaction times are obtained with both catalysts when the KOH concentration is

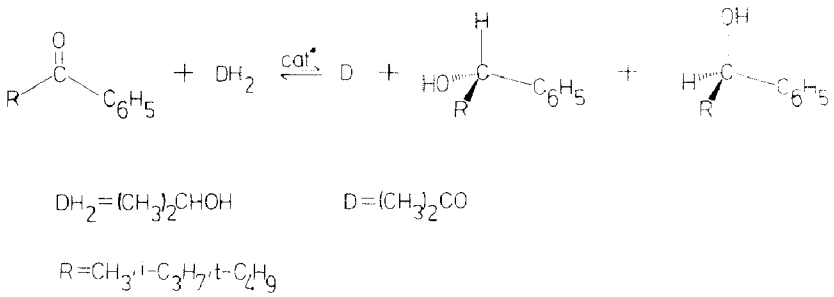

Scheme 1.

Table 6

Reduction of t-butyl phenyl ketone by propan-2-ol; catalyst precursors: [Ir(COD)*S*(+)PPEI(I)] (I), [Ir(COD)*R*(−)PPEI]ClO_4 (III) [a]

Catalyst precursor	[KOH]/[Ir]	Conv.(%)	Time(min)	e.e.(%)
I	1.5	98	120	66.0 *S*(−)
I	2.0	95	105	66.0 *S*(−)
III	1.5	91	120	50.0 *R*(+)
III	2.0	99	75	51.5 *R*(+)

[a] Reaction conditions: [cat. prec.] = 1.6×10^{-4} *M*; [sub.]/[cat. prec.] = 1000; [propan-2-ol]/[sub.] = 81.5; propan-2-ol = 125 ml; *T* 83° C.

Table 7

Reduction of t-butyl phenyl ketone by propan-2-ol; catalyst precursor [Ir(COD)*S*(+)PPEI(I)] [a]

H_2O (% vol.)	Conv. (%)	Time (min)	e.e. (%)
0	92	105	67.0 *S*(−)
0.5	94	105	73.5 *S*(−)
1.0	94	120	78.0 *S*(−)
1.5	94	120	80.0 *S*(−)
2.0	94	120	80.0 *S*(−)
5.0	90	240	80.0 *S*(−)

[a] Reaction conditions: see Table 6; [KOH]/[Ir] = 1.5.

measured. The catalytic activity of and, particularly the asymmetric induction by, the two complexes, depend on the amount of water. As can be seen from Table 7, the [Ir(COD)(PPEI)I] complex becomes less active but more selective with increasing water content, and a maximum value of 80% is reached at 1.5% of water. The corresponding tetracoordinated derivative shows the opposite effect (Fig. 4).

Contrasting behaviour of the two precursors I and III is seen also when the substrate concentration is varied. Thus increasing the [sub.]/[Ir] ratio, in the case of I causes a sharp decrease in the optical induction, but with III causes an increase in both the activity and selectivity, reaching an average rate of 1660 cycles/h and an enantiomeric excess of 63.5% at [sub.]/[Ir] ratio = 3000 (Fig. 5). This is the best result achieved in the reduction of t-butyl phenyl ketone using III as catalyst precursor.

Table 8 summarizes the data obtained using I and II as catalyst precursors and methyl, isopropyl, and t-butyl phenyl ketones as substrates. Both complexes show the pattern previously observed in the case of [Ir(COD)(PPEI)]ClO_4 [6]; the reaction rate and the selectivity increase on going from methyl to t-butyl phenyl ketone, i.e. with increasing steric hindrance and electrophilicity of the substrate. The latter can

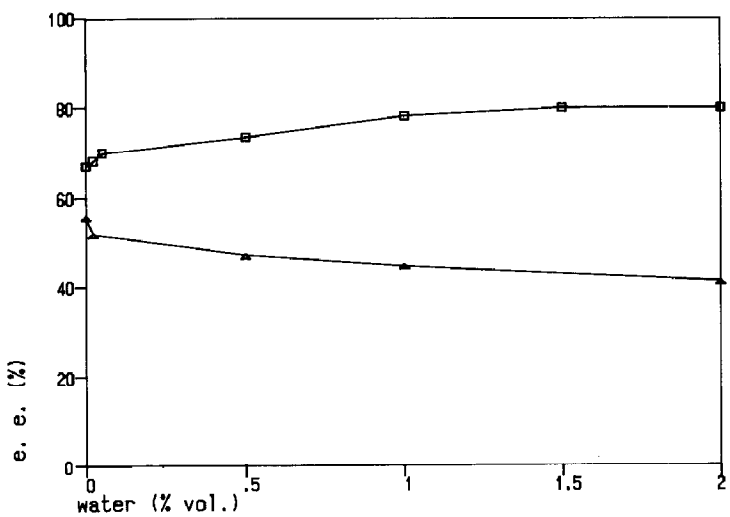

Fig. 4. Influence of water concentration on enantiomeric excess. □ = [Ir(COD)(PPEI)I]. Reaction conditions: see Table 7. △ = [Ir(COD)(PPEI)]ClO_4. Reaction conditions: see Table 6, [KOH]/[Ir] = 2.

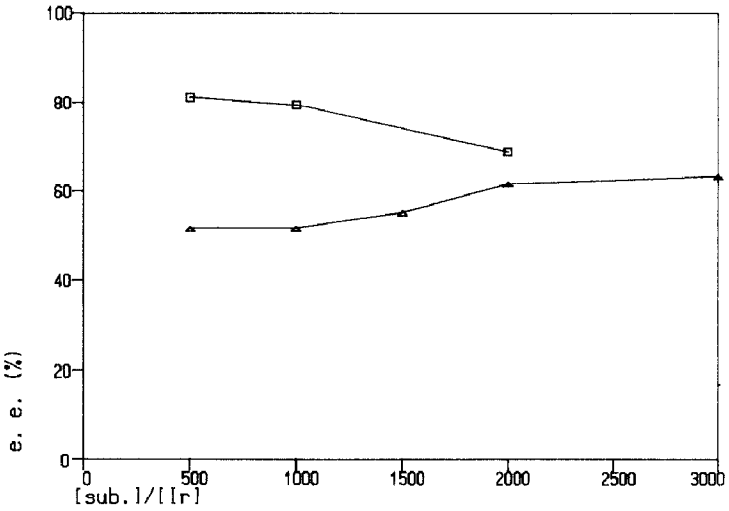

Fig. 5. Influence of [sub.]/[Ir] ratio on enantiomeric excess. □ = [Ir(COD)(PPEI)I]. Reaction conditions: see Table 6; [KOH]/[Ir] = 2; H_2O (%vol.) = 2.0. △ = [Ir(COD)(PPEI)]ClO_4. Reaction conditions: [cat. prec.] = 1.6×10^{-4} *M*; H_2O (% vol.) = 0; propan-2-ol = 125 ml; *T* 83° C.

be related, at least for this reaction, to the redox potential $E°$ [21] of the ketone/alcohol couple [6].

Moreover, as can be seen from Tables 8 and 9, in the case of both the iodo and perchlorate complexes, the PPEI derivatives are more selective than the corresponding APPEI derivatives. Similar behaviour has been observed in hydrosilylation

Table 8

Reduction of alkyl phenyl ketones by propan-2-ol; catalyst precursors: [Ir(COD)*S*(+)PPEI(I)] (I), [Ir(COD)*S*(+)APPEI(I)] (II) [a]

Catalyst precursor	Ketone	$E°$ [b] (mV)	Conv. (%)	$\bar{r}$ [c] (cycles/h)	e.e. (%)
I	$CH_3COC_6H_5$	118	88	160	36.5 *S*(−)
I	i-$C_3H_7COC_6H_5$	125	91	183	52.0 *S*(−)
I	t-$C_4H_9ClOC_6H_5$	169	94	472	79.5 *S*(−)
II	$CH_3COC_6H_5$	118	92	153	19.5 *S*(−)
II	i-$C_3H_7COC_6H_5$	125	92	154	27.0 *S*(−)
II	t-$C_4H_9COC_6H_5$	169	96	382	42.0 *S*(−)

[a] Reaction conditions: see Table 6; [KOH]/[Ir] = 2; H_2O (%vol.) = 2.0. [b] Redox potential alcohol/ketone couple [21]. [c] Average rate between 0 and the reported conversion.

Table 9

Reduction of t-butyl phenyl ketone by propan-2-ol; catalyst precursor: [Ir(COD)NNR*]ClO_4 [a]

NNR*	Conv. (%)	Time (min)	e.e. (%)
S(+)PPEI	95	90	56.0 *S*(−)
S(+)APPEI	97	45	29.5 *S*(−)

[a] Reaction conditions: see Table 6; [KOH]/[Ir] = 2.0; H_2O (% vol.) = 0.

Table 10

Reduction of t-butyl phenyl ketone by propan-2-ol; catalyst precursor: [Ir(COD)*S*(+)PPEI(I)] [a]

$[I^-]/[Ir]$	Conv. (%)	Time (min)	e.e. (%)
1.0	94	120	79.5 *S*(−)
2.0	95	105	82.0 *S*(−)
3.0	91	240	84.0 *S*(−)

[a] Reaction conditions: see Table 8.

reactions catalyzed by the Rh^I derivatives with the same chiral ligands [7]. In contrast, complexes I and II show the same activity (Table 8), whereas IV is more active than III (Table 9).

The overall data indicate that the neutral pentacoordinate species I and II are considerably more enantioselective than the corresponding cationic tetracoordinated derivatives III and IV. Since the iodo derivative could dissociate to give a cationic species, as depicted in eq. 1, the reaction was also performed in the presence of NaI in order to shift the equilibrium towards the more enantioselective neutral species.

$$[IrI(NNR^\star)(ROH)_2] \rightleftharpoons [Ir(NNR^\star)(ROH)_3]^+ + I^- \quad (1)$$

Data in Table 10 indicate that increasing the $[I^-]/[Ir]$ ratio improves the asymmetric induction, a maximum value of 84% enantiomeric excess being reached of $[I^-]/[Ir] = 3.0$. This result is, to our knowledge, the highest optical yield achieved up to now in catalytic asymmetric reduction of non-functional ketones in both hydrogenation and hydrogen transfer reactions.

The catalytic cycle previously proposed for the cationic derivatives [5,6] is assumed to operate also with the neutral iodo-species. The catalyst is assumed to be a neutral pentacoordinate derivative of Ir^I. Both the bidentate nitrogen donor ligand and the iodide are coordinated to the metal ion; solvent molecules occupy the two free coordination positions (Fig. 6).

The reaction of coordinated propan-2-ol with KOH gives the isopropoxy derivative, and the ketone coordinates the metal through the oxygen atom after displacement of a solvent molecule. Hydrogen transfer from the donor to the acceptor molecule follows, and it is assumed to be the rate- and selectivity-determining step of the cycle, and to proceed through a six-membered cyclic transition state, involving the direct transfer of the hydrogen atom from the isopropoxy group to the electrophilic centre of the substrate.

The complex $[Ir(NNR^\star)I(OR)(ketone)]^-$ can exist in two limiting geometries: square pyramidal and a trigonal bipyramidal. The most favoured isomers (Fig. 7) could be those having donor and acceptor molecules in equatorial positions at about 120°; in this case in fact, a lower angular distorsion is required on going to the transition state.

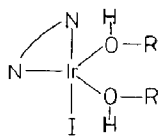

Fig. 6. The assumed catalytically active species.

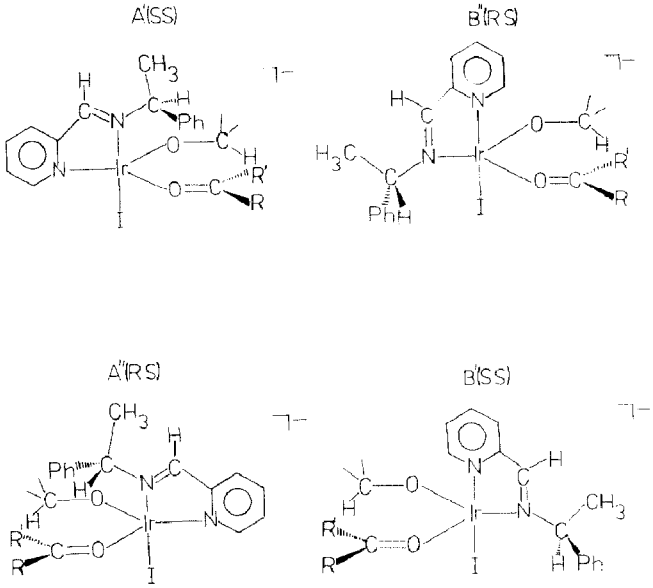

Fig. 7. Most significant geometrical isomers of [Ir(PPEI)I(OR)(ketone)]$^-$.

Moreover every geometric isomer should be present in solution as a diastereoisomeric pair, since these species contain two chiral centres: the asymmetric carbon atom of the ligand (configurationally stable) and the pentacoordinate iridium atom (configurationally labile).

The diastereoisomers A'(*SS*) and A''(*RS*), according to a suggestion by Wojcicki [22], when in a complex two or more chiral centres are present, the metal designa-

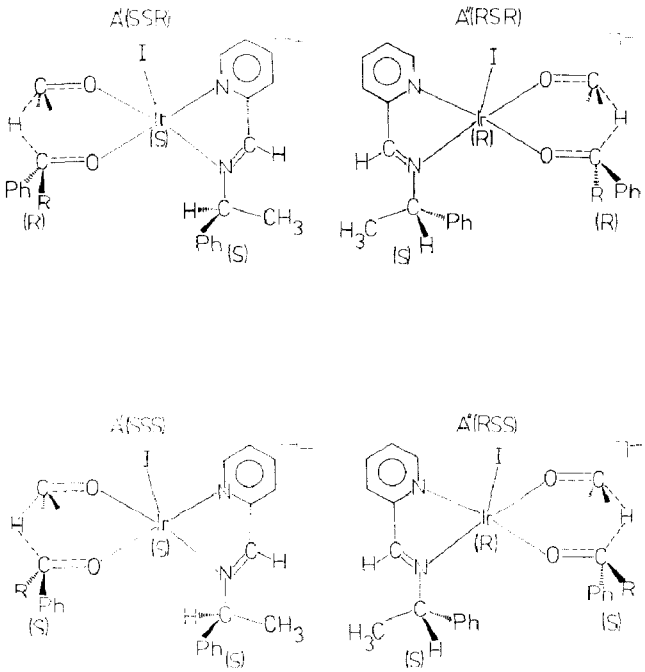

Fig. 8. Possible transition states for species A'(*SS*) and A''(*RS*).

tion precedes that of carbon), must be mainly responsible for the observed enantio-discrimination, when account is taken of the shorter distance between the chiral centre of the ligand and the prochiral one of the substrate compared to that in the diastereoisomers B′(*SS*) and B″(*RS*). For the diastereoisomeric species in solution, depicted in Fig. 7, only the most stable conformation has been considered [23], i.e. the one in which the methyl group of the asymmetric carbon atom eclipses the double imine C=N bond. Hydrogen transfer can occur on the *Re* or *Si* face of coordinated ketone, and so four transition states, originating from the two diastereoisomers A′(*SS*) and A″(*RS*), can be considered. Since, when the *S*(+) ligand is used, the S(−) alcohol predominates always hydrogen transfer on the Re face of the substrate is favoured, and thus the transition states A′(*SSS*) and A″(*RSS*) must be those preferred (Fig. 8).

In these transition states there could be a stabilizing interaction between the phenyl group of the substrate and that of the asymmetric carbon atom of the ligand, since these two groups are close. Such interaction could be mainly responsible for the observed high enantioselectivities. In the transition states A′(*SSR*) and A″(*RSR*) originating from hydrogen transfer on the *Si* face of the ketone, these interaction should be absent, and there could be a destabilizing interaction between the alkyl substituent of substrate and the phenyl group of the asymmetric carbon atom of the ligand. Such a destabilizing interaction should increase with increase in the steric hindrance by the alkyl group. In accord with this suggestion, an increase of optical yield is observed going from methyl to t-butyl derivatives with both precursors (Table 9).

From the structural data for complexes I and II, the lower selectivity of II can be related to an increase of the distance between the phenyl groups of the ligand and the substrate in the transition states A′(*SSS*) and A″(*RSS*) formed from II. Such an increase would involve weakening of the stabilizing interactions between the two phenyl rings, with consequent loss of selectivity.

Conclusions

Use of neutral pentacoordinate [Ir(COD)(PPEI)I] species as catalyst precursor leads to higher enantioselectivities than those previously observed by use of the corresponding cationic tetracoordinated [Ir(COD)(PPEI)]ClO_4 species. In particular the new catalytic system shows a good rate of reduction and an optical yield of 84% in the case of the rather hindered substrate t-butyl phenyl ketone, which is only very slowly reduced when other catalyst systems are used.

Higher enantiomeric excesses could be obtained with complexes similar to those used in this work by optimizing the attractive interactions, which are mainly responsible for enantioselectivity, between the chiral centre of the ligand and the prochiral centre of the substrate.

A further increase in the asymmetric induction might be obtained by using terdentate nitrogen donor ligands with C_2 symmetry, such as the diimines which can be synthesized by condensation of pyridine-2,6-dialdehyde with two molecules of a chiral primary amine, and oxazolines of the type reported by Nishiyama et al. [9]. Synthesis of these ligands and their related complexes is in progress in our laboratory.

Experimental

Chemicals

Pyridine-2-aldehyde (Carlo Erba) was distilled under reduced pressure before use. The commercially available 2-acetylpyridine (Carlo Erba), *R*(+)- and *S*(−)-1-phenylethylamine (Merck) was used as received.

Propan-2-ol (Carlo Erba) was distilled over CaO and stored under an inert atmosphere. Methyl phenyl ketone (Riedel), isopropyl phenyl ketone (Aldrich), and t-butyl phenyl ketone (Fluka) were washed with a 5% aqueous KOH solution, dried over anidrous Na_2SO_4, distilled at reduced pressure, and stored under argon.

Synthesis of the ligands and complexes

The Schiff bases were prepared by the published procedure [13,7].

The complexes were prepared and filtered under an argon stream using deaerated solvents, dried in vacuo at room temperature, and stored under an inert atmosphere. The analytical data are listed in Table 11. The complexes $[Ir(COD)Cl]_2$ and $[Ir(COD)(PPEI)]ClO_4$ were prepared by published methods [24,5]. To prepare $[Ir(COD)(NNR^{\star})]ClO_4$ ($NNR^{\star}$ = *S*(+)APPEI (**1**), *R*(−)APPEI (**2**)) and $[Ir(COD)(NNR^{\star})I]$ ($NNR^{\star}$ = *S*(+)PPEI (**3**), *R*(−)PPEI (**4**), *S*(+)APPEI (**5**), *R*(−)APPEI (**6**)), 0.33 g (0.5 mmol) of $[Ir(COD)Cl]_2$ were suspended in CH_3OH (6.0 ml) and treated with a slight excess of the ligand to give a deep blue-violet solution; after 20 min stirring addition of solid $NaClO_4$ or NaI caused immediate precipitation of the microcrystalline complexes. The products were filtered off and washed with water and then ligroin (b.p. 75–120 °C). The complexes were recrystallized under argon at room temperature from $CHCl_3$/ligroin (75–120 °C) 1/1.5 (**3**, **4**) and from CH_2Cl_2/ligroin (75–120 °C) 1/1.5 (**5**, **6**).

Transfer hydrogenation procedure

Appropriate amounts of the complexes were suspended in 125 ml of propan-2-ol in a three-necked flask and oxidized overnight with a stream of dry air at room temperature. The orange solutions were deaerated by heating under reflux in an argon stream. Appropriate amounts of deaerated solution of KOH in propan-2-ol were added at reflux. After 10 min an appropriate amount of deaerated water or aqueous NaI was added. After 30 min, the deaerated substrate (neat) was added to the boiling solution from a dropping funnel kept at 65 °C. The progress of the

Table 11

Elemental analyses of the complexes

Formula	Found (Calc.)(%)		
	C	H	N
$[Ir(COD)S(+)APPEI]ClO_4$	43.2(44.2)	4.60(4.52)	4.26(4.48)
$[Ir(COD)R(-)APPEI]ClO_4$	43.1(44.2)	4.53(4.52)	4.02(4.48)
[Ir(COD)*S*(+)PPEI(I)]	41.0(41.5)	4.04(4.04)	4.39(4.40)
[Ir(COD)*R*(−)PPEI(I)]	40.9(41.5)	4.39(4.04)	4.30(4.40)
[Ir(COD)*S*(+)APPEI(I)]	41.4(42.4)	4.12(4.33)	4.38(4.30)
[Ir(COD)*R*(−)APPEI(I)]	41.8(42.4)	4.26(4.33)	4.25(4.30)

Table 12

Maximum rotatory power and sign-configuration relationship for the alcohols obtained

Alcohol	$[\alpha]_D^T$ (°)	T (°C)	Medium	Relation sign-conf.	Ref.
$CH_3CH(OH)C_6H_5$	43.6	25	neat	$R(+)$	25, 26
i-$C_3H_7CH(OH)C_6H_5$	47.7	20	c 6.8 [a]	$R(+)$	27, 28
t-$C_4H_9CH(OH)C_6H_5$	27.8	27	c 2.7 [b]	$R(+)$	26

[a] Diethyl ether. [b] $CHCl_3$.

reaction was monitored by GLC analysis of samples withdrawn under argon. (The samples were immediately oxidized by air and the reaction stopped.) The final solution was treated with a suitable amount of aqueous CH_3COOH.

Propan-2-ol was evaporated off and the liquid product was isolated by distillation at reduced pressure. The composition of the distillate was determined by GLC.

The optical rotations of the alcohols (neat or solution) were measured at the temperature corresponding to maximum specific rotation. The optical purities, calculated from the values for pure enantiomers listed in Table 12, were corrected for the presence of unchanged starting material and for the optical purities of the ligands. GLC analyses were performed on DANI 6800 instrument equipped with a Shimadzu C-RIA data processor. Rotatory powers were measured with a Perkin–Elmer 241 micropolarimeter.

Acknowledgements

We thank MPI (60%) Rome and C.N.R. for financial support.

References

1 J. Bakos, I. Tóth, S. Heil and L. Markó, J. Organomet. Chem., 279 (1985) 23.
2 R. Spogliarich, J. Kaspar, M. Graziani and F. Morandini, J. Organomet. Chem., 306 (1986) 407.
3 P. Kvintovics, B.R. James and B. Heil, J. Chem. Soc. Chem. Commun., (1986) 1810.
4 G. Zassinovich and F. Grisoni, J. Organomet. Chem., 247 (1983) C24.
5 G. Zassinovich, C. Del Bianco and G. Mestroni, J. Organomet. Chem., 222 (1981) 323.
6 G. Zassinovich and G. Mestroni, J. Mol. Cat., 42 (1987) 81.
7 H. Brunner, B. Reiter and G. Riepl, Chem. Ber., 117 (1984) 1330.
8 H. Brunner and A. Kürzinger, J. Organomet. Chem., 346 (1988) 413.
9 H. Nishiyama, H. Sakuguchi, T. Nakamura, M. Horihata and K. Itoh, VI International Symposium on Homogeneous Catalysis, August 1988, Vancouver, Canada, 7-53.
10 C. Botteghi, G. Chelucci, G. Chessa, G. Delogu, S. Gladiali and F. Soccolini, J. Organomet. Chem., 304 (1987) 217.
11 S. Gladiali, G. Chelucci, G. Chessa, G. Delogu and F. Soccolini, J. Organomet. Chem., 327 (1987) C15.
12 F. Vinzi, G. Zassinovich and G. Mestroni, J. Mol. Cat., 18 (1983) 359.
13 F. Nerdel, K. Becker and G. Kresze, Chem. Ber., 12 (1956) 2862.
14 D. Rogers, Acta Crystall., A, 37 (1981) 734.
15 International Tables for X-ray Crystallography, Vol. IV, Kynoch Press, Birmingham, U.K. 1974.
16 R.S. Cahn, C. Ingold and V. Prelog, Angew. Chem., Int. Ed. Eng., 5 (1966) 385.
17 C. Lecomte, Y. Dusausoy, J. Protas, J. Tirouflet and A. Dormond, J. Organomet. Chem., 73 (1974) 67.
18 K. Stanley and M.C. Baird, J. Am. Chem. Soc., 97 (1975) 6598.
19 H. Brunner, G. Riepl, I. Bernal and W.H. Ries, Inorg. Chim. Acta, 112 (1986) 65.

20 I. Bernal, W. Ries, H. Brunner and D.K. Rastogi, J. Organomet. Chem., 290 (1985) 353.
21 H. Adkins, R.M. Elofson, A.G. Rossow and C.C. Robinson, J. Am. Chem. Soc., 71 (1949) 3622.
22 P.R. Rohrwig and A. Wojcicki, Inorg. Chem., 13 (1974) 2457.
23 H. Brunner and D.K. Rastogi, Bull. Soc. Chim. Belg., 89 (1980) 883.
24 J.L. Herdé and C.V. Senoff, Inorg. Nucl. Chem. Lett., 7 (1971) 1029.
25 E.L. Eliel, J. Am. Chem. Soc., 71 (1949) 3970.
26 F. MacLeod, F.J. Welch and M.S. Mosher, J. Am. Chem. Soc., 82 (1960) 876.
27 D.J. Kram and J.E. Mc Carty, J. Am. Chem. Soc., 79 (1957) 2866.
28 R.H. Pikard and J. Kenyon, J. Chem. Soc., 99 (1911) 45.